

#### IV. FINITE-DIFFERENCE SOLUTIONS OF LAPLACE EQUATION

The use of finite-difference methods enables one to solve numerically many boundary value problems involving partial differential equations of elliptic type for which explicit analytic solutions are not available. In 1940's, these methods were primarily used for manual computations as described by Southwell<sup>(18)</sup>, Shortley and Weller<sup>(19)</sup>, and Allen<sup>(20)</sup>.

The development of high-speed digital computers has made feasible the numerical solution by iterative methods of some partial differential equations since 1950. The iterative methods involve successively applied local corrections to improve an approximate solution. However, these iterative methods are routinized in conformity with the requirements of automatic computers.

In using numerical methods, the region to be studied is divided into a grid of mutually orthogonal lines having a finite number of intersections as shown in fig. 7. We shall use the finite-difference equivalent of Laplace's equation and numerical methods for calculating the potentials at the intersections from a knowledge of the conditions on the boundary of the region.

In deriving the finite-difference approximation of Laplace's equation, to be used in calculating the

potentials for this project, we shall assume that there are no variations of the potential along the y-coordinate:

$$\frac{\partial^2 \Phi}{\partial x^2} + \frac{\partial^2 \Phi}{\partial z^2} = 0 \text{ ----- (4.1)}$$

A convenient way to evaluate the second partial derivatives of  $\Phi$  with respect to the x- and z- coordinates is to expand the potential about the point (x,z) using a Taylor series:<sup>(21)</sup>

$$\Phi(x+h,z) = \Phi(x,z) + h \frac{\partial \Phi(x,z)}{\partial x} + \frac{h^2}{2} \frac{\partial^2 \Phi(x,z)}{\partial x^2} \text{ --(4.2)}$$

$$\Phi(x-h,z) = \Phi(x,z) - h \frac{\partial \Phi(x,z)}{\partial x} + \frac{h^2}{2} \frac{\partial^2 \Phi(x,z)}{\partial x^2} \text{ --(4.3)}$$

where eq.(4.2) is the forward difference expansion, and eq.(4.3) is the backward difference expansion.

By adding eq.(4.2) and (4.3), and rearranging, we have:

$$\frac{\partial^2 \Phi(x,z)}{\partial x^2} = \frac{\Phi(x+h,z) + \Phi(x-h,z) - 2\Phi(x,z)}{h^2} \text{ ----- (4.4)}$$

The second partial derivative with respect to z-coordinate can be obtained in the same way. So eq.(4.1) can be expressed in the approximate form:

$$\Phi(x,z) = \frac{1}{4} [ \Phi(x+h,z) + \Phi(x-h,z) + \Phi(x,z+h) + \Phi(x,z-h) ] \text{ ----- (4.5)}$$

This equation is called the 5-point difference equation and is shown in fig. 8.

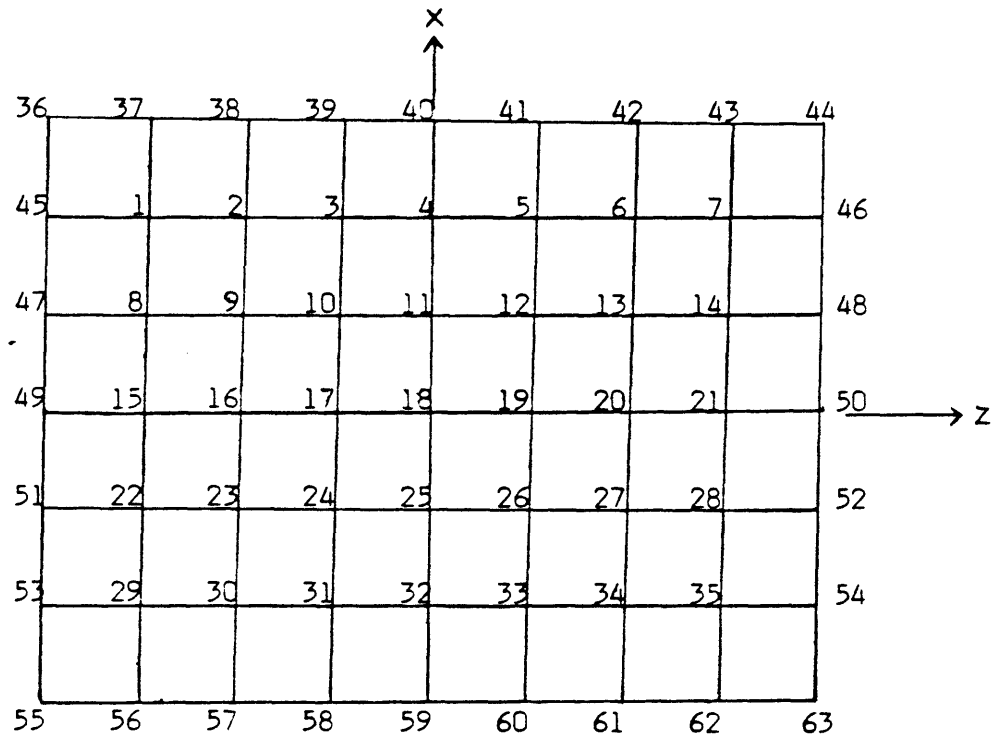


Fig. 7 Grid for difference equation solution.

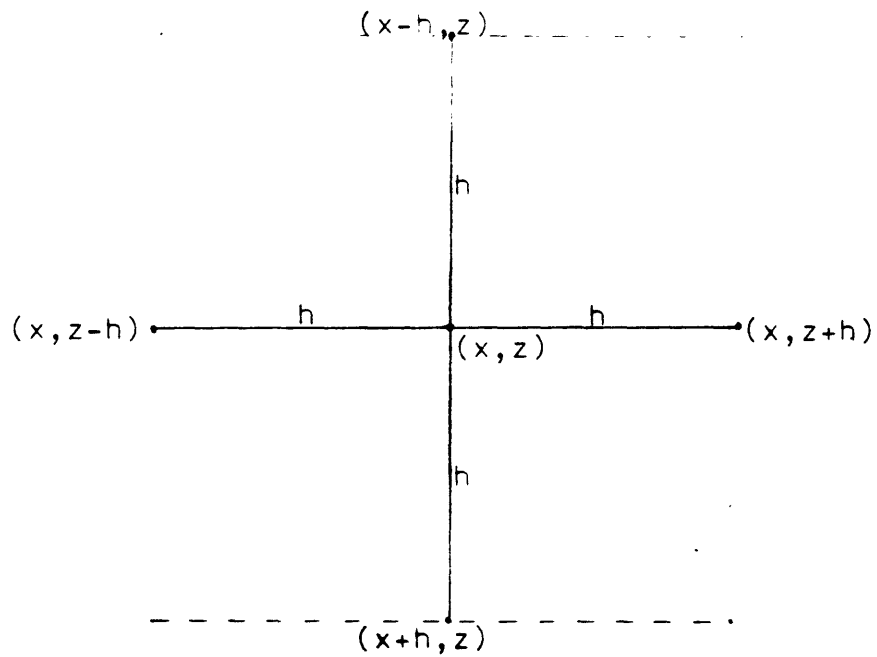


Fig. 8 5-point difference, mesh size:  $h$ .

Any numerical method used for solving a differential equation necessarily involves the replacement of the continuum of points on the boundary and in the interior of the region by a discrete set of net points. The method which has been previously given for handling Laplace's equation is an iterative procedure due to Liebmann, and called the 'Liebmann method'. In addition to demonstrating the feasibility of such a routine, we are interested in studying empirically the rate of convergence of various iterative methods for solving the difference equation.

For problems involving a large number of net points the usual iterative method, commonly referred to as the 'Liebmann method', or as the 'Gauss-Seidel method', converges extremely slowly. It is of considerable advantage to use a modification of this method developed independently by Frankel<sup>(22)</sup> and by Young<sup>(23)</sup>, and called the 'extrapolated Liebmann method' or the 'successive over-relaxation method'.

Both the 'Liebmann method' and the 'extrapolated Liebmann method' for solving Laplace's equation use the same iterative process and in its simplest form the lattice is scanned in the direction along successive rows. The iterative process may be written as:

$$\bar{x}_{j,k}^{n+1} = \bar{x}_{j,k}^n + \mathcal{L} [ \bar{x}_{j-1,k}^{n+1} + \bar{x}_{j+1,k}^n + \bar{x}_{j,k-1}^{n+1} + \bar{x}_{j,k+1}^n - 4\bar{x}_{j,k}^n ]$$

----- (4.6)

for the interior points, and

$$\bar{x}_{j,k}^{n+1} = b_{j,k} \text{ ----- (4.7)}$$

for the boundary points.

The  $\bar{x}$ -value so corrected is used in all subsequent operations in that iterative steps. It may thus be termed a 'continuous substitution method'. The 'Liebmann method' and the 'extrapolated Liebmann method' are described in the next two sections.

#### 1. Liebmann method (Gauss-Seidel method)

In this method,  $\mathcal{L}$  is equal to  $\frac{1}{4}$  in eq.(4.6), then eq.(4.6) becomes

$$\bar{x}_{j,k}^{n+1} = \frac{1}{4} [ \bar{x}_{j-1,k}^{n+1} + \bar{x}_{j+1,k}^n + \bar{x}_{j,k-1}^{n+1} + \bar{x}_{j,k+1}^n ] \text{ --- (4.8)}$$

A square net is laid down over the region and one starts by assigning approximate values to the interior points and known values to the boundary points. Then by choosing an ordering of the net points and scanning over the lattice through eq.(4.8), we can generate  $\bar{x}_{j,k}^{n+1}$ . For example, using the order in which the points are numbered in fig. 7, and replacing each  $\bar{x}_i^n$  by the average of the

four neighboring values we get an improved value  $\Phi_i^{n+1}$  and using this new value immediately for the improvement of the succeeding point  $\Phi_{i+1}^{n+1}$ , e.g. in fig. 7,

$$\Phi_{13}^{n+1} = \frac{1}{4} [ \Phi_{12}^{n+1} + \Phi_{14}^n + \Phi_6^{n+1} - \Phi_{20}^n ] \text{ ----- (4.9)}$$

The function  $\Phi_i^{n+1}$  is then closer to the solution of the difference equation than was  $\Phi_i^n$ . Iteration of this process will then converge to a solution of the Laplace's equation which is as close to the true solution as may be desired. Usually the smaller the mesh size  $h$ , the better the approximation one can reach.

## 2. Extrapolated Liebmann method (successive over-relaxation method)

The only difference between the 'Liebmann method' and the 'extrapolated Liebmann method' is  $\alpha$ . In this method,  $\alpha$  is greater than  $\frac{1}{4}$ . We can rewrite eq.(4.6) in the following form:

$$\Phi_{j,k}^{n+1} = \Phi_{j,k}^n + \frac{\beta}{4} [ \Phi_{j-1,k}^{n+1} + \Phi_{j+1,k}^n - \Phi_{j,k-1}^{n+1} + \Phi_{j,k+1}^n - 4\Phi_{j,k}^n ] \text{ ----- (4.10)}$$

where  $\beta$  is known as 'relaxation factor', satisfying the condition  $1 \leq \beta \leq 2$ , and

$$\Phi_{j-1,k}^{n+1} + \Phi_{j+1,k}^n + \Phi_{j,k-1}^{n+1} + \Phi_{j,k+1}^n - 4\Phi_{j,k}^n$$

is defined as a 'residue'  $R^n$ .

At each step in a calculation, the potential and residue are listed for each point of the net which is not on the boundary. When all residues approach zero, eq.(4.10) is satisfied and final solution is reached.

The rapidity of convergence can be greatly increased by the introduction of the 'relaxation factor'. For a rectangular region the optimum value of  $\beta$  can be computed exactly and its use results in a saving of a factor of 10 in the number of iteration.

It was shown by Frankel<sup>(22)</sup> for the case of Laplace's equation for the rectangle, and by Young<sup>(23)</sup> for self-adjoint elliptic difference equation, the optimum value of  $\beta$ ,  $\beta_0$ , is given by<sup>(24)</sup>

$$\beta_0 = 1 + \frac{\lambda}{[1 + \sqrt{1 - \lambda}]^2} \text{ ----- (4.11)}$$

For any rectangle it is easy to compute  $\lambda$  exactly and for a unit square with mesh size h, we have

$$\lambda = \cos^2(\pi h) \text{ ----- (4.12)}$$

It was also shown by Young<sup>(24)</sup> that if  $\beta$  is slightly larger than  $\beta_0$ , then the increase in the iteration number N is relatively small, but if  $\beta$  is less than  $\beta_0$ , then there is a much larger increase in N.

## V. RESULTS AND DISCUSSIONS

### 1. RESULTS

In this special topic, we used the 'successive over-relaxation method' to solve the Laplace's equation. Fig. 9 shows the region we studied. Since the voltage due to the kicker voltage at infinity is zero, we assumed that the "infinity" was at  $18h$  from the anode and  $12h$  from the kicker electrodes. The mesh size  $h$  of this region is  $\frac{1}{18}$  because the ratio of the length of the  $x$ - and  $z$ -coordinate is  $18:18$ . Using eq. (4.11) and (4.12), we can estimate the optimum relaxation factor to be  $\omega_0 = 1.704$ .

For these calculations, we also assumed that the charge density in the region was zero so that there is no effect on the electric field lines due to the free charge and the application of Laplace's equation is suitable. Otherwise we must use Poisson's equation instead.

#### (1) Calculations of voltages

The flowchart shown in fig. 10 is a description of the program (appendix I) written to solve eq. (4.10). Table 1 (appendix II) shows the voltage values of  $V(x,z)$ . The upper and the lower half are symmetric except for a minus sign in the lower half because of  $+5KV$  on the upper electrode and  $-5KV$  on the lower electrode.



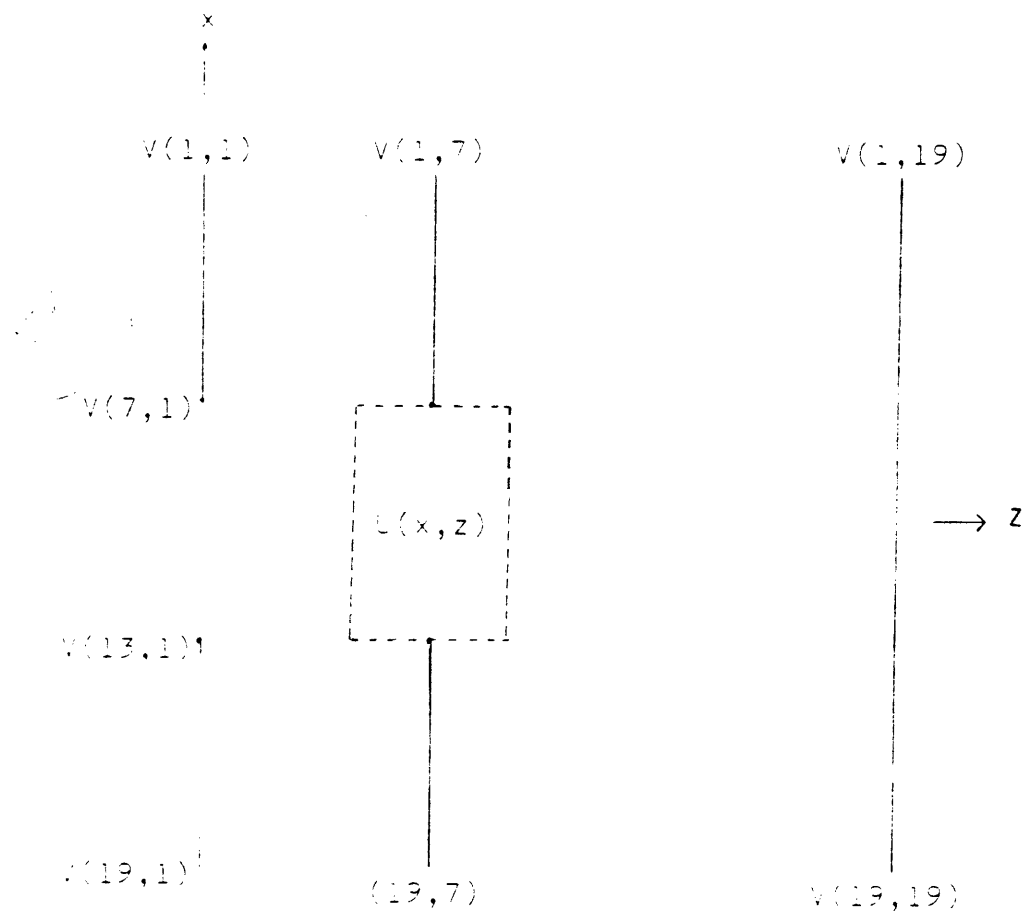


Fig. 9

$V(x,z) : 19 \times 19$  ;  $V(7,5)=U(1,1)$ ,  $V(13,5)=U(31,1)$

$U(x,z) : 31 \times 21$  ;  $V(7,9)=U(1,21)$ ,  $V(13,9)=U(31,21)$

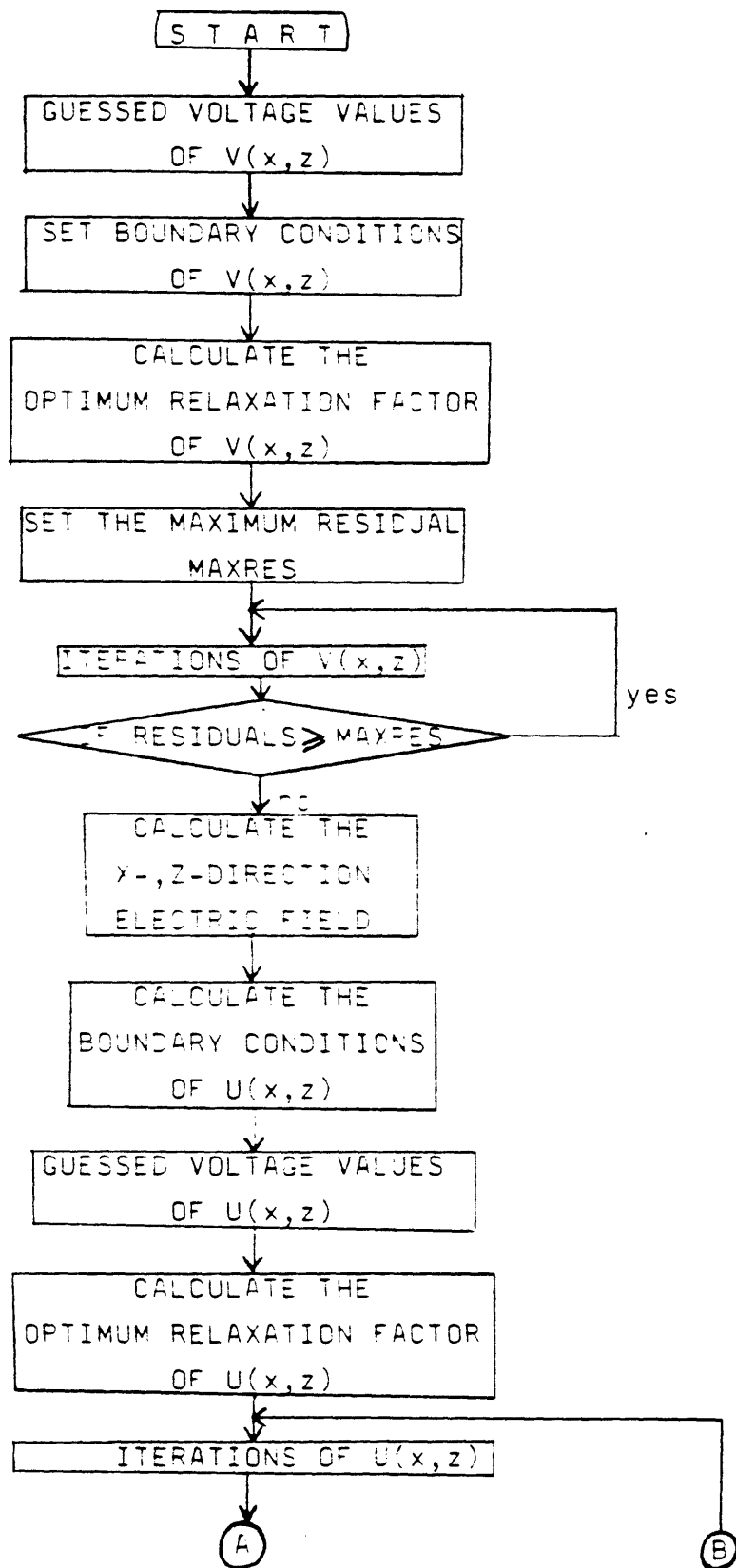
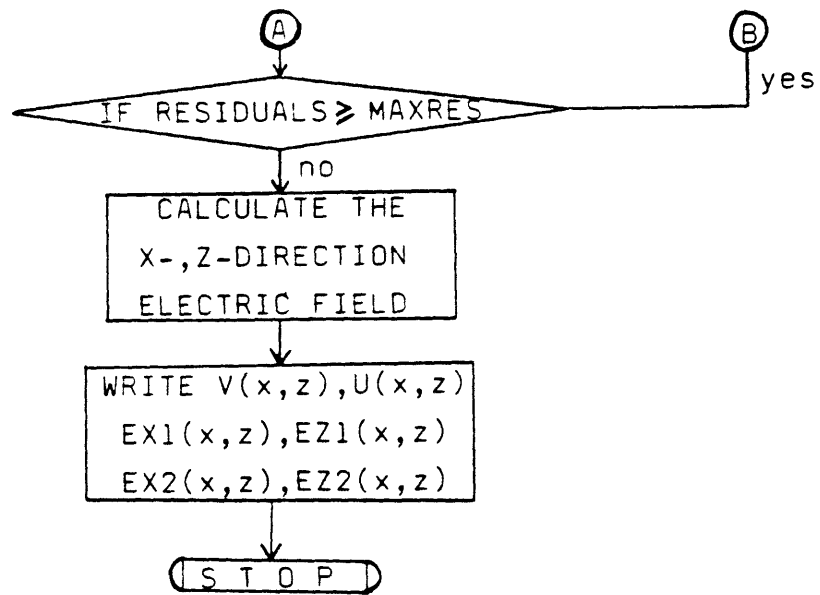


Fig.10 Flowchart



END

Fig. 10 Flowchart (continued)

We selected the rectangular region shown dotted in fig. 9 which was of great importance due to the electric field values there and designated this region as  $U(x,z)$ . For the boundary conditions of this region, the distance between two values of  $V(x,z)$  is very small. From the mathematical point of view, we can calculate the boundary values of  $U(x,z)$  linearly. The ratio of the width and the length of  $U(x,z)$  region is 20:35, and hence the mesh size of this region is  $\frac{1}{20}$ , using this mesh size we can compute the optimum relaxation factor of this region  $\omega_0 = 1.729$ . The voltage values shown in table 2 are there for the region  $U(x,z)$ .

## (2) Calculations of electric fields

The definition of electric field is the negative of the gradient of the potential:

$$\vec{E} = -\text{grad } \Phi = - \left( \frac{\partial \Phi}{\partial x} \vec{a}_x + \frac{\partial \Phi}{\partial y} \vec{a}_y + \frac{\partial \Phi}{\partial z} \vec{a}_z \right) \text{ -----(5.1)}$$

From the Taylor series expansion in eq.(4.2) and eq.(4.3), and by subtracting eq.(4.3) from eq.(4.2), we obtained:

$$\frac{\partial \Phi(x,z)}{\partial x} = \frac{\Phi(x+h,z) - \Phi(x-h,z)}{2h} \text{ -----(5.2)}$$

in which  $h = \frac{5}{6}$  mm. Eq.(5.2) is called the central-difference equation.

The electric field in x-direction is

$$\bar{E}_x = - \frac{\Phi(x+h,z) - \Phi(x-h,z)}{2h} \text{ ----- (5.3)}$$

and in z-direction is

$$\bar{E}_z = - \frac{\Phi(x,z+h) - \Phi(x,z-h)}{2h} \text{ ----- (5.4)}$$

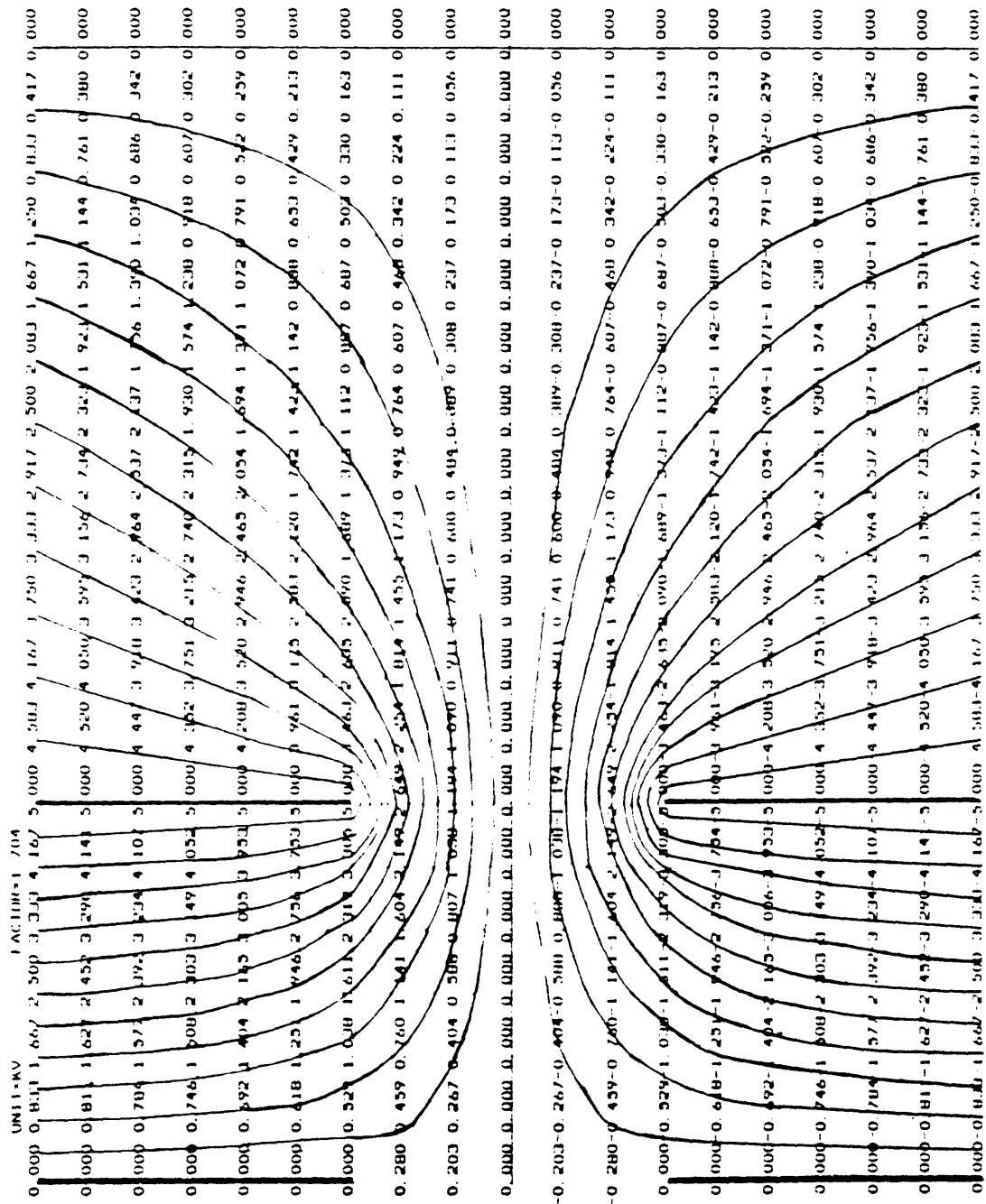
For  $V(x,z)$ , we calculated the electric field in the path where the width is the width of the aperture between two anode electrodes and the length is  $12h$  from the anode.

We used eq.(5.3) and (5.4) to calculate the electric fields of both  $V(x,z)$  and  $U(x,z)$ . These results are shown in table 3, 4, 5.

### (3) Constant potential and electric fields

From the voltage values of  $V(x,z)$  shown in table 1, we plotted the equipotential lines by hands which were shown in fig. 11. The electric field lines were also drawn by the technique of graphical field mapping and a few examples are shown in fig. 12.

Fig. 13 and 14 show the computer plots of x- and z-components of the electric field as a function of  $r$  at various distances from the accelerating anode electrodes. The electric field along the axial z-direction at constant value of  $r$  were also plotted and shown in fig. 15 and 16.



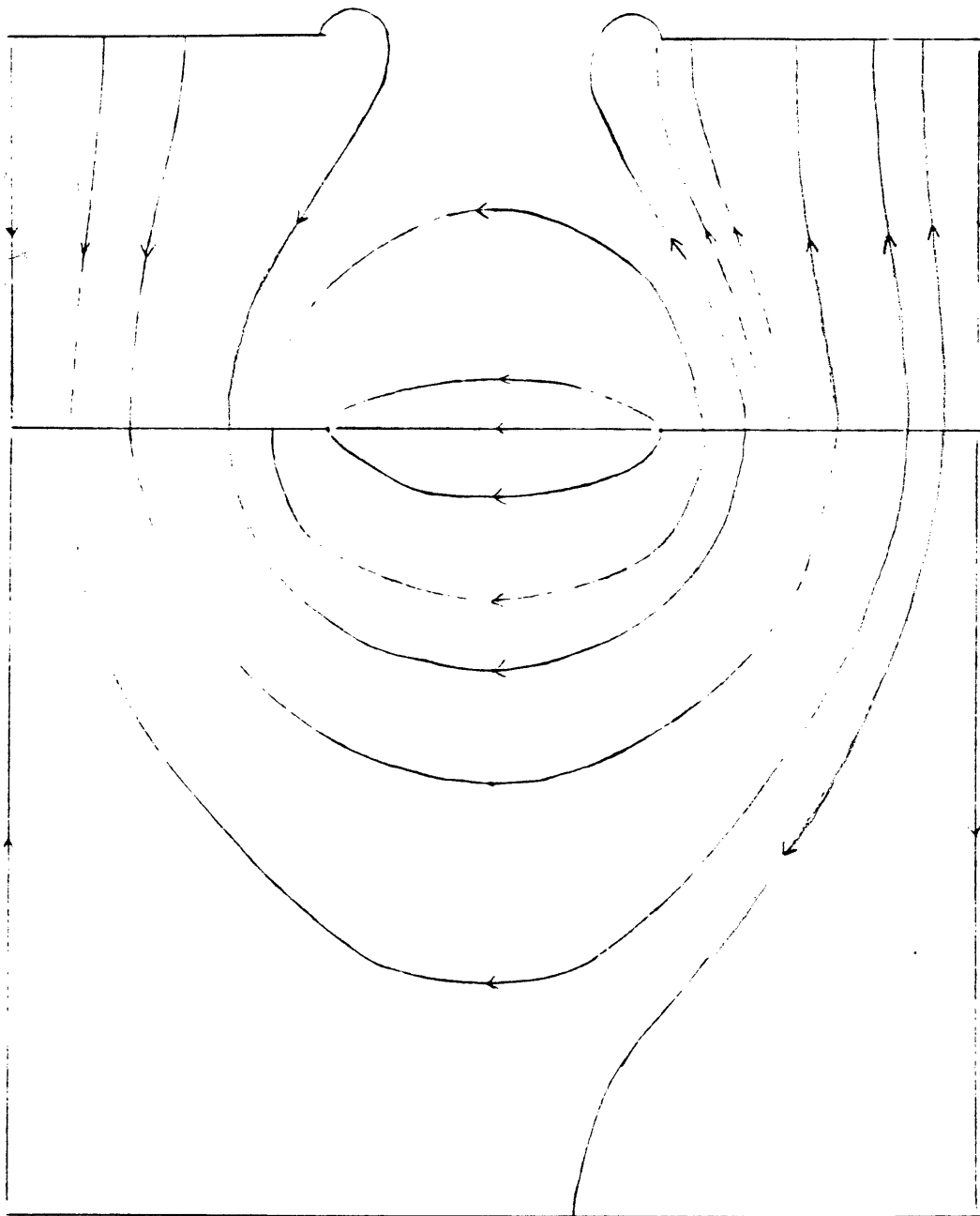


Fig. 12 Examples of electric field lines by graphical mapping

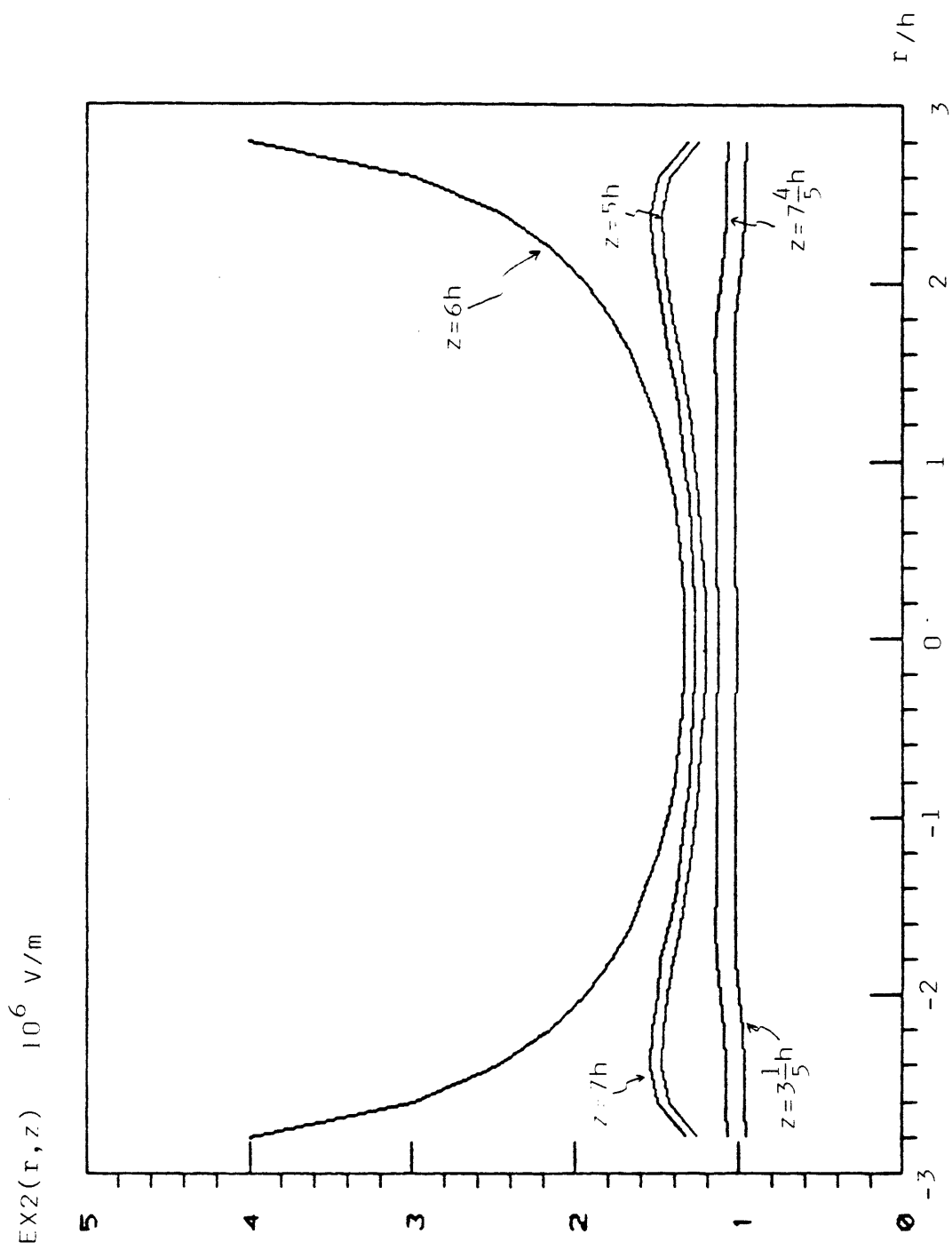


Fig. 13  $EX2$  as a function of  $r$  with various distances from anode



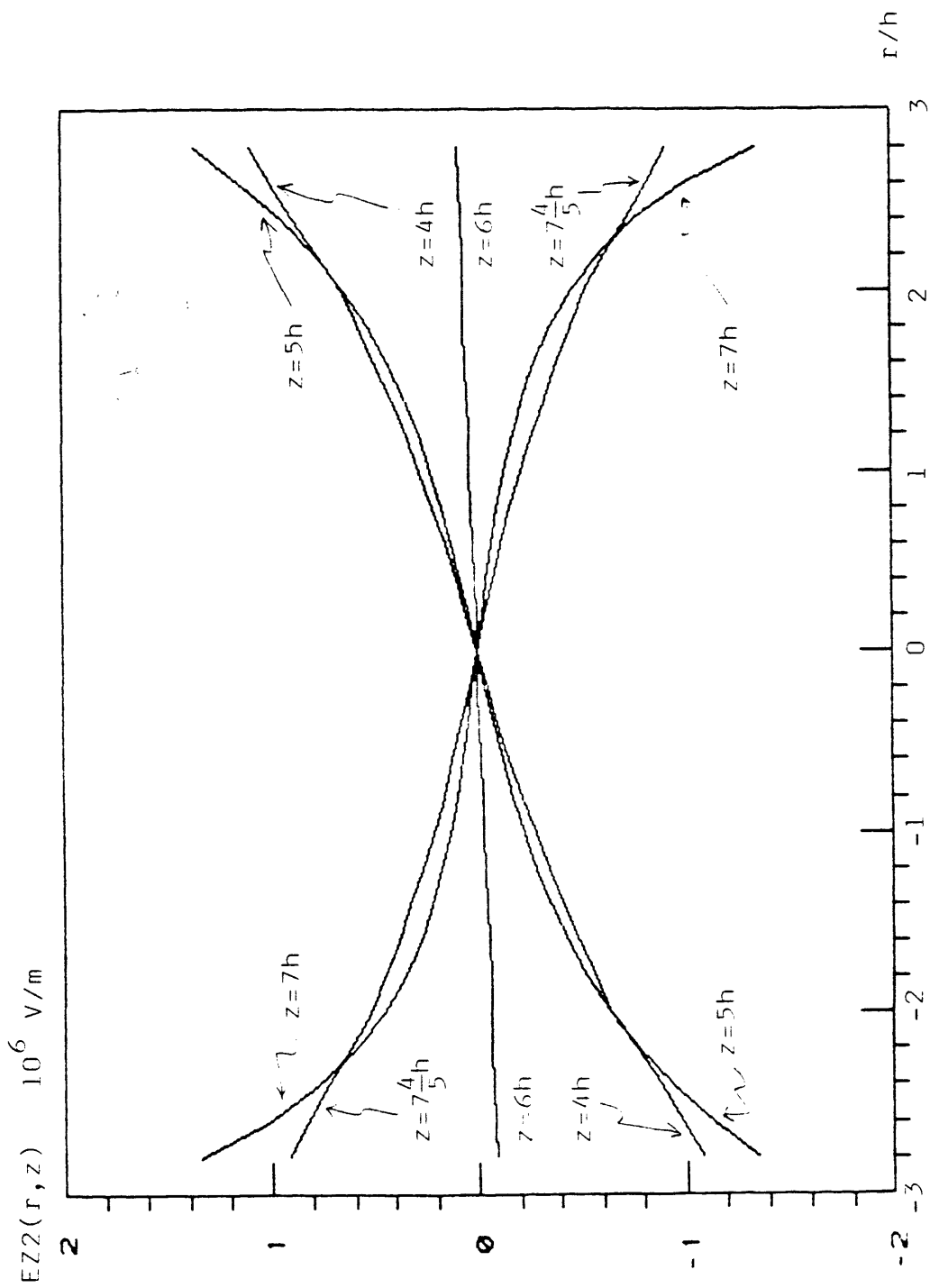


Fig. 14  $EZ2$  as a function of  $r$  with various distances from anode

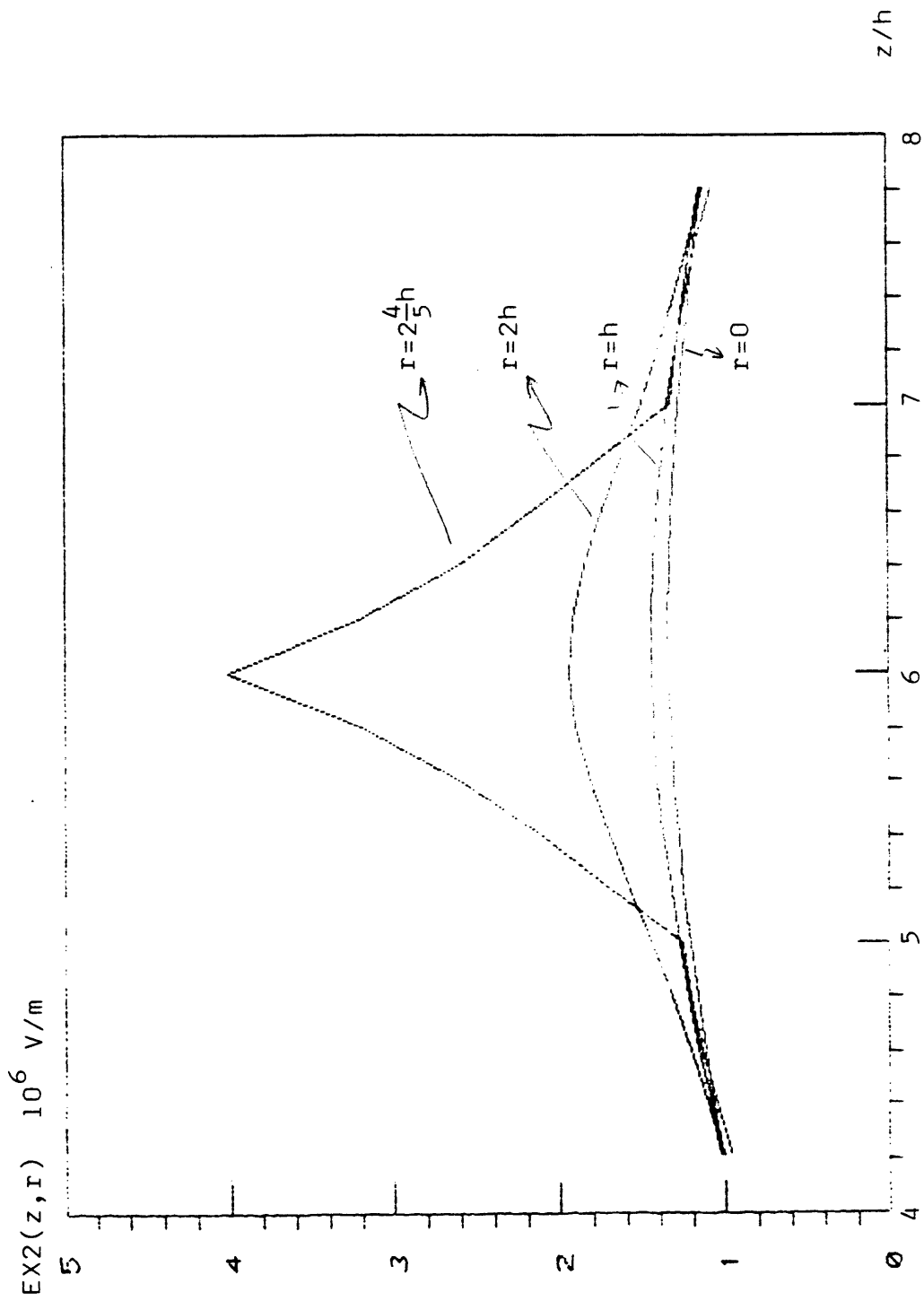


Fig. 15  $EX2$  as a function of axial direction at various constant values of  $r$

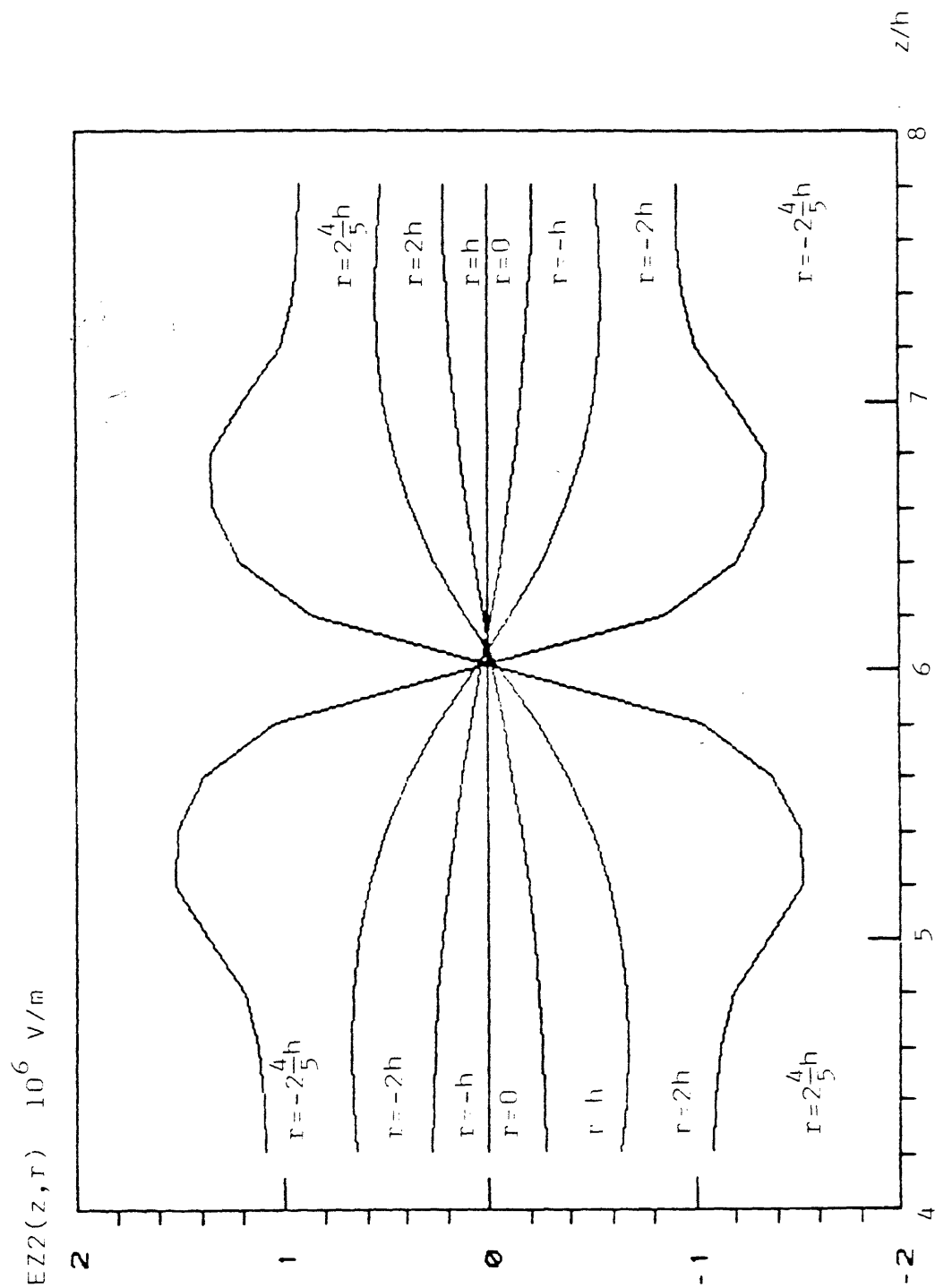


Fig. 16  $E_z$  as a function of axial direction at various constant values of  $r$

16. A. T. Lin and K. R. Chu, "A Study of the Saturated Output of a  $TE_{01}$  Gyrotron Using an Electromagnetic Finite Size Particle Code," Int. J. Electronics, vol. 53, No. 6, pp. 659-671, 1982.
17. J. F. Hoburg and J. L. Davis, "A Student-oriented Finite Element Program for Electrostatic Potential Problems," IEEE Trans. Education, vol. E-26, No. 4, pp. 138-142, 1983.
18. R. V. Southwell, "Relaxation Methods in Theoretical Physics," Oxford Univ. Press, 1946.
19. G. Shortley and R. Weller, "The Numerical Solution of Laplace's Equation," J. Appl. Phys., vol. 9, pp. 334-344, 1938.
20. D. N. Allen, "Relaxation Methods," McGraw-Hill Book Co., New York, 1954.
21. S. J. Farlow, "Partial Differential Equations for Scientists and Engineers," 1982.
22. S. Frankel, "Convergence Rates of Iterative Treatment of Partial Differential Equations," Math. Table and Other Aids to Computation, vol. 4, pp. 65-75, 1950.
23. D. M. Young, "Iterative Methods for Solving Partial Difference Equations of Elliptic Type," Trans. Amer. Math. Soc., vol. 76, pp. 92-111, 1954.
24. D. M. Young, "ORDVAC Solutions of the Dirichlet Problems," J. Association for Computing Machinery, vol. 2, No. 3, pp. 137-161, 1955.
25. S. D. Conte and Carl de Boor, "Elementary Numerical Analysis, An Algorithmic Approach," 3rd Ed., p. 395, McGraw-Hill Book Co., 1980.